Published in final edited form as:
Int J Biochem Cell Biol. 2007 ; 39(12): 2303–2313.

The Intracellular Form of Human MAGP-1 Elicits a Complex and Specific Transcriptional Response

Fernando Segade[a,1,*], **Nobuyasu Suganuma**[b,2], **Josyf C. Mychaleckyj**[a,3], and **Robert P. Mecham**[c]

a *Center for Human Genomics, Wake Forest University School of Medicine, Winston-Salem, NC 27157, USA*

b *Department of Biochemistry, Wake Forest University School of Medicine, Winston-Salem, NC 27157, USA*

c *Department of Cell Biology and Physiology, Washington University School of Medicine, St. Louis, MO 63110, USA*

Abstract

Microfibril-associated glycoprotein-1 (MAGP1) is found associated with microfibrils in the extracellular matrix (ECM). In humans, MAGP1 is expressed as two alternatively spliced isoforms: MAGP1A, the extracellular microfibril-associated form; and MAGP1B, an exclusively intracellular isoform derived from the skipping of exon 3. The biological function of MAGP1B is unknown. We performed gene expression profiling to study the cellular response to MAGP1B using whole-genome genechips. We found that MAGP1B specifically induces the expression of genes linked to cell adhesion, motility, metabolism, gene expression, development and signal transduction. Versican, a gene product involved in the structure and functional regulation of the ECM, showed the highest up-regulation in response to MAGP1B. These studies suggest a dual role for MAGP1, with extracellular MAGP1A involved in ECM function, and intracellular MAGP1B modulating the expression of genes that function in cell adhesion, migration and control of ECM deposition.

Keywords

MAGP1; Microfibrils; Alternate transcripts; microarray; matricellular; intracrin

1. Introduction

Microfibrils are ubiquitous structures in the ECM of most tissues, particularly elastic tissues, bone, and cartilage (Mecham and Davis, 1994). Microfibrils make an essential contribution to the structural integrity of tissues, anchor cells to matrix components through cell adhesion motifs (Robinson and Godfrey, 2000), sequester growth factors in the ECM (Charbonneau et al., 2004), and signal cells by interacting with cell surface receptors (Sakamoto et al., 1996). Microfibril-associated glycoproteins (MAGPs) are low molecular weight components of the microfibrils (Gibson et al., 1991). MAGP1 is a 183-amino acid protein with two domains: an

*Corresponding author. Department of Anatomy and Cell Biology, University of Pennsylvania School of Dental Medicine, 240 South 40th Street, Philadelphia, PA 19104. Tel.: +1 215 898 8994; fax +1 215 573 2324. E-mail address: segade@dental.upenn.edu (F. Segade)..
[1]Current address: Department of Anatomy and Cell Biology, University of Pennsylvania School of Dental Medicine, Philadelphia, PA 19104, USA
[2]Current address: Department of Surgery, Yokohama City University, Yokohama, Kanagawa 236-0004, Japan.
[3]Current address: Department of Public Health Sciences, University of Virginia, Charlottesville, VA 22908, USA.

amino terminal half enriched in proline and glutamine residues; and a carboxy terminal half with a 54-amino acid region that targets MAGP1 to the ECM (Segade et al., 2002). Extracellular MAGP1 is known to bind to tropoelastin, collagen VI, fibrillin, decorin, and biglycan (Brown-Augsburger et al., 1994; Finnis and Gibson, 1997; Reinboth et al., 2002; Trask et al., 2000; Werneck et al., 2004). MAGP1 interacts with and facilitates the shedding of Notch (Miyamoto et al., 2006).

MAGP1 is encoded by the Mfap2 (from Microfibril-associated protein 2) gene located in chromosome 1p31 in human (Faraco et al., 1995) and 4qD3 in mouse (Chen et al., 1993). Ortholog sequences are present in amphibians and teleost fishes (Segade et al., 2002). In mammals the gene is split in 9 exons of which exon 1 is non-coding. Analysis of the human gene expression databases (Karolchik et al., 2003) shows that MAGP1 mRNA expression is highest in blood vessels, lung, and placenta and, in general terms, in organs rich in smooth muscle (e.g. uterus, prostate).

Canonical splicing of the human MAGP1 pre-mRNA gives rise to a 1.3-kb transcript. Alternative splicing originates species-specific splice variants of MAGP1 (Segade et al., 2000). In humans, the alternate MAGP1B mRNA originates from an exon-skipping event that prevents the incorporation of exon 3 into the processed transcript. The MAGP1B transcript is present in normal tissue RNA with differential expression patterns (Segade et al., 2000). Interestingly, MAGP1B message was found in cells that do not deposit an ECM, like peripheral leukocytes, suggesting that MAGP1 could possess a second biological role independent from its function in the ECM. The skipped exon codes for 30 amino acids that include a portion of the signal peptide including the cleavage site, indicative of an intracellular location (Segade et al., 2000). This hypothesis was later verified by the observation that a GFP-tagged MAGP1B accumulates in the cytoplasm and is not secreted (Segade et al., 2002).

In order to define the intracellular role of MAGP1B we performed a transcriptome analysis of the cellular response to MAGP1B. As sources of RNA for microarray analysis we developed stably transfected human cell lines expressing each of the human MAGP1 alternate isoforms. We found that MAGP1B modulates a unique set of genes that suggest a role of MAGP1B in cell processes that involve cell migration, adhesion and control of ECM deposition.

2. Materials and Methods

2.1. Cell culture

The human osteosarcoma cell line SAOS-2 (ATCC HTB-85) (Fogh et al., 1977) was purchased from the American Type Culture Collection and routinely maintained in Dulbecco's modified Eagle's medium (DMEM, Cambrex) supplemented with 10% fetal bovine serum (Invitrogen), 10 units/ml of penicillin, and 10 μg/ml of streptomycin. Cells were cultured in a standard humidified incubator at 37°C in a 5% CO_2-95% O_2 atmosphere.

2.2. Recombinant plasmids

Construction of the chimeric MAGP-V5-6His fusion proteins was carried out in the pcDNA3.1/V5-His plasmid (Invitrogen). Genes cloned into this vector are expressed under the control of the CMV promoter. The MAGP1A-V5 vector with the full length (183 amino acids) human MAGP1A was constructed by amplification using the forward HM-5 (5′-TTAGAATTCGCCATGAGAGCTGCCTAC-3′) and reverse HM-3 (5′-TTATCTAGAGCAGCTCCCACAGCTCCT-3′) primers and human MAGP1A cDNA (Segade et al., 2000) as a template to generate a 560-bp amplification product. The MAGP1B-V5 plasmid containing the human MAGP1B coding sequence (153 amino acids) was constructed by amplification with the HM-5 and HM-3 primers using the human EST clone

H27217 template (Genome Systems) to generate a 470-bp amplification product. PCR fragments were gel-purified, and digested with EcoRI and XbaI for ligation to pcDNA3.1/V5-His. The integrity of the constructs was verified by sequencing with the T7 and BGH primers (Invitrogen) and analyzed with Chromas software. Plasmids were routinely purified from bacterial cultures with the Qiagen EndoFree Maxi DNA purification kit.

2.3. Generation of MAGP1 stable transfectants in SAOS-2 cells

SAOS-2 cells at ~90% confluence were transfected with 5 μg of the appropriate plasmid using 5 μl of the LipofectAMINE 2000 (Invitrogen) transfection reagent for 6 h. Transfectants were selected by culture in growth medium supplemented with 700 μg/ml of Geneticin (Invitrogen) for 17 days. Geneticin-resistant cells were pooled and RNA was extracted to verify the expression of the appropriate MAGP1 transgene mRNA by conventional RT-PCR.

2.4. RNA isolation

Total RNA was extracted from SAOS-2 stable transfectants using the isothiocyanate-acid phenol method (Chomczynski and Sacchi, 1987), and further purified by chromatography using the Qiagen RNeasy system according to the manufacturer's instructions. The integrity of the RNA was ascertained by electrophoretic separation of 2 μg of total RNA in 1.2% agarose-formaldehyde denaturing gels and visualized by ethidium bromide staining.

2.5. cDNA synthesis and conventional PCR analysis

Single-stranded cDNA was synthesized from 1 μg of total RNA in a final volume of 20 μl containing 20 mM Tris-HCl (pH 8.4), 50 mM KCl, 5 mM $MgCl_2$, 500 μM dNTP mix, 50 μg random hexamers and 200 units of Super Script III Reverse Transcriptase (Invitrogen) at 50° C for 50 min followed by inactivation of the reverse transcriptase at 70°C for 10 min and hydrolysis of the template RNA with 2 units of RNase H (Invitrogen) at 37°C for 30 min. After digestion with 2 units of RNase H, 1 μg of cDNA was used as template for PCR. mRNA samples incubated in the absence of reverse transcriptase served as negative controls. For conventional PCR, the cDNA equivalent of 200 ng of total SAOS-2 RNA was amplified with 0.4 μM each of the appropriate primers (Table 1) in a 25-μl volume containing 20 mM Tris-HCl (pH 8.4), 50 mM KCl, 1.5mM $MgCl_2$, 200 μM dNTP mix, and 2 units of Titanium Taq DNA polymerase (Clontech). After an initial denaturation at 95°C for 1 min, 30 cycles of amplification were performed at 95°C for 30 s, 60°C for 30 s and 68°C for 30 s, followed by 3 min at 68°C as an additional extension step. PCR products were then separated in 2% agarose gels and visualized by ethidium bromide staining.

2.6. Indirect Immunofluorescence

For indirect immunofluorescence detection, cultures of SAOS-2 cells, plated on microscopy coverslips, were washed with phosphate-buffered saline and fixed with cold methanol. Nonspecific immunoreactivity was blocked with 1% fat-free milk in phosphate-buffered saline for 1 h at room temperature. Coverslips were then incubated with monoclonal anti-V5 primary antibody (Invitrogen) for 1 h at room temperature, followed by several washes in blocking solution and a second incubation with Alexa 488-conjugated goat anti-mouse secondary antibody (Santa Cruz Biotechnology) for 30 min. Slides were washed and mounted on microarray slides. Fluorescence was examined with a Leitz DM-RBE fluorescence microscope equipped with a single-channel CCD camera. Images acquired with ×10-×40 objectives and a ×10 eyepiece were recorded and manipulated using Openlab 3.5.1 software.

2.7. Microarray hybridization experiments

Total RNA was purified from SAOS-2 transfectants as described above. RNA labeling and hybridization were carried out at the Wake Forest University Affymetrix Microarray Core

Facility according to the recommended protocols. Briefly, biotin-labeled RNA was hybridized to Affymetrix Human Genome U133A probe arrays, stained with streptavidin-PE conjugate (Molecular Probes), and the fluorescence intensities were measured with an Affymetrix GeneScanner laser confocal scanner, according to the manufacturer's instructions. Two independent transfection-hybridization experiments were performed for each expression vector.

2.8. Statistical analysis of the hybridization data

Raw data from the hybridization experiments was processed using the Affymetrix Microarray Suite Version 5.0 to extract transcript detection calls and intensities. All arrays were globally scaled to the same target intensity and scaling factors checked for consistency according to standard Affymetrix protocols. To smooth within-transfectant biological and empirical variation, the independent transfectant array data sets were analyzed as separate groups of replicates. Additional information on statistical methods can be found in (Cobb et al., 2004). We combined the individual array MAS 5.0 detection statistics (gene transcript present/absent call and p-value) into an overall statistic for each group to classify gene transcripts (i.e., probe sets on the array) as present or absent at the group level. Changes in expression levels of gene transcripts were detected through two separate tests. Transcripts with Absolute Change in gene expression are those detected as present in one array but not in the other (Fisher omnibus test of present-absent or absent-present $p<0.01$). Transcripts with Relative Change in gene expression (detected as 'present' in the control and both MAGP1A- and MAGP1B-expressing transcriptomes) were assigned to the 'Confident' category if the expression change $p<0.00004$ or $p>0.99996$ (increase or decrease respectively) corresponding to a maximum of 1 false positive gene expression change call per array comparison. Transcripts that meet this criterion and had a fold expression change of 1.5 or higher were scored with 'Highest Confidence'. Genes were mapped to probes sets and classified by molecular function (ontology classification) (Harris et al., 2004) using Expression Analysis Systematic Explorer (EASE; http://david.niaid.nih.gov/david) and Netaffyx (http://www.affymetrix.com) analyses.

2.9. Quantitative real-time PCR

Results from the microarray analysis were validated by quantitative real-time PCR. PCR primer sequences for target genes were designed from mRNA sequences deposited in Genbank with PrimerBank (http://pga.mgh.harvard.edu/primerbank/index.html) (Wang and Seed, 2003). Primers were designed for products in the 150–200 bp range, preferentially from sequence closer to the 5′ end of each gene, and with forward and reverse primers on different exons (Table 1). PCR conditions were checked and optimized using a range of annealing temperatures. Real time quantitative RT-PCR was carried out in 96-well plates using an ABI PRISM 7000 Sequence Detection System. Total RNA extracted from stably transfected SAOS-2 cells and purified through RNeasy columns was treated with RNase-free DNase (Promega) to avoid spurious amplification from copurifying genomic DNA. First-strand cDNA was synthesized from 1 μg of total RNA with 2.5 μM random hexamers as primers and 60 units of Multiscribe reverse transcriptase (Applied Biosystems). The reaction (50 μl) was incubated at 25°C for 10 min, followed by incubation at 48°C for 30 min and 95°C for 5 min. cDNA were used as template for quantitative real-time PCR with the SYBR green chemistry detection method. Amplification mixtures totaling 50 μl per reaction contained 4 μl of template, 1× SYBR Premix Ex Taq master mix buffer (Takara Mirus Bio), 1× ROX passive reference dye, and 0.2 μM forward and reverse primers. Cycling conditions followed the manufacturer's recommendations for a 3-step PCR protocol with a 10-sec initial denaturation at 95°C followed by 40 cycles at 95°C for 5 sec, 55–60°C for 20 sec and 72°C for 30 sec, with quantification detection at the 72°C extension step. A final quantified denaturing step from 55°C to 95°C produced a melting curve to determine product specificity. Universal 18S rRNA endogenous control primers and probe sets were purchased from Applied Biosystems. All samples were

run in triplicate, with a no-template negative control. Levels of mRNA were calculated from the threshold cycle number (C_t) during the exponential phase of the PCR amplification. The C_t was established as the cycle number at which the amount of amplified target reached a fixed fluorescence threshold. The mean (± SEM) C_t values of the experimental triplicates were calculated for each gene and sample. Samples with more than 10% of variation within the triplicate were retested or excluded. The difference between the C_t values of the target gene and the endogenous control was determined to calculate $\Delta C_t = C_{t\,(\text{target gene})} - C_{t\,(\text{reference})}$. For each target gene, normalization was performed against the values in the SAOS-C line, with each SAOS-C ΔC_t value subtracted from the ΔC_t in SAOS-MAGP1A or SAOS-MAGP1B to obtain the $\Delta\Delta C_t$ (Livak and Schmittgen, 2001). Finally, the relative expression R of each target gene in the SAOS-MAGP1A or SAOS-MAGP1B lines was calculated as $R = 2^{-\Delta\Delta Ct}$. The statistical significance of differences in expression levels was determined with the multiple t-test. The significance level was defined as $p < 0.05$.

3. Results

3.1. Characterization of MAGP1A and MAGP1B Stable Transfectants in SAOS-2 Cells

To generate stable transfectants in the human SAOS-2 osteosarcoma cell line, MAGP1A or MAGP1B coding sequences were subcloned into the pcDNA3.1/V5-6His vector. Empty pcDNA3.1/V5-6His vector was used to generate the negative control cell line SAOS-C. Expression of the splice form-specific mRNAs from G418-resistant clones was ascertained by conventional RT-PCR using primers derived from exons 2 (HM5) and 6 (HM3) of the human gene. As shown in Fig. 1A, a 336-bp amplification product was obtained from the SAOS-MAGP1A cell line which, upon sequencing, was confirmed to correspond to the MAGP1A sequence. Similarly, RT-PCR using SAOS-MAGP1B RNA produced a 246-bp amplification product that corresponds to the exon 3-skipped MAGP1B (Fig. 1A). Relative levels of MAGP1A and MAGP1B were assessed by real-time PCR (Fig. 1B). MAGP1B mRNA expression in the SAOS-MAGP1B line is ~37% of the level of the MAGP1A mRNA in the SAOS-MAGP1A cells.

Evidence that the transfectants express the appropriate MAGP1 protein and not just their mRNAs can be seen in the results of immunofluorescence experiments using monoclonal antibodies against the V5 tag present in the recombinant proteins (Fig. 1C). In SAOS-MAGP1A cells, V5 immunostaining was clearly visible in a perinuclear golgi cap, consistent with the passage of MAGP1A through the secretory pathway (Fig. 1C, left panel). A more diffuse fluorescence consistent with a cytoplasmic localization was observed in SAOS-MAGP1B cells (Fig. 1C, right panel). No V5 staining was seen in SAOS-C or in untransfected SAOS-2 cells (not shown).

We conclude that MAGP1A and MAGP1B are expressed stably at the mRNA and protein levels in human SAOS-2 cells.

3.2. Complex and specific transcriptional response to MAGP1B

Biotin-labeled complementary RNA was synthesized to probe the Affymetrix U133A Human Genome oligonucleotide chip platform which contains 22,283 sets of probes. All microarray experiments were performed with two independently isolated transfected cell lines using independently prepared RNA samples to probe two individual genechips for each line to account for experimental variability. Raw hybridization data were processed to extract probe set signal intensities and detection calls. In order to isolate the MAGP1B-specific response and to eliminate non-specific alterations in gene expression due to transfection effects and protein over-expression, we first identified the statistically significant changes between SAOS-

MAGP1A or SAOS-MAGP1B relative to MAGP1-C. A second subtraction analysis identified the genes up- or down-regulated only in the SAOS-MAGP1B line.

There were a total of 2253 statistically significant changes (2208 up-regulated, 45 down-regulated) in gene expression in SAOS-MAGP1B cells relative to SAOS-C, while 3388 statistically significant changes were observed in SAOS-MAGP1A cells (3281 up-regulated, 107 down-regulated) relative to SAOS-C. After selection of those changes taking place *uniquely* in SAOS-MAGP1B relative to SAOS-C, and not in SAOS-MAGP1A, we discovered 75 changes that were statistically significant, specific for MAGP1B and above a threshold of 1.5-fold variation. Out of these, 67 genes were up-regulated, whereas the expression of 8 genes was lower in SAOS-MAGP1B than in SAOS-C.

The statistically significant changes in biochemical and cellular pathways in response to over-expression of MAGP1B according to EASE analysis are summarized in Table 2, arranged into 11 categories together with the peak ratio. Excluding the “Uncharacterized gene product” category (14 genes), the broad categories “Metabolism” (10 genes), “Gene expression” (9 genes), “Signal transduction” (8 genes), and “Development” and “Intracellular Structure” (7 genes each), comprise the bulk of the up-regulated genes. The much smaller number of down-regulated genes (8 genes) was classified into 7 categories.

The highest up-regulation was found for CSPG2, encoding the chondroitin sulfate proteoglycan, versican (peak ratio 2.76); whereas the most significant down-regulation was observed for CSTF2, Cleavage stimulation factor, subunit 2 (peak ratio 0.55), one of the factors required for 3′-end cleavage of mammalian pre-mRNAs (Takagaki et al., 1992).

3.3. Validation of the genechip results by real-time PCR

Validation of the microarray results by real-time PCR of selected genes is shown in Fig. 2. As sources of RNA we used a set of transfected SAOS-2 cells generated independently of the cell lines used in the genechip experiments in order to provide a more robust analysis. We chose the four genes uniquely induced by MAGP1B with the highest peak ratios: CSPG2 (peak ratio 2.76), CDC42EP3 (peak ratio 2.43), ITGA4 (peak ratio 2.15), and PTCH (peak ratio 2.00). Real-time PCR data were processed according to the ΔΔCt value method (Livak and Schmittgen, 2001), and normalized for equal amounts of initial RNA by amplification of 18S rRNA. Since microarray analysis may not always be able to distinguish among alternatively spliced forms of a particular gene, the detected signal may actually represent the sum of the relative contributions of all the variants. In our case, the mRNA for CSPG2 (versican) is alternatively spliced into four variants (termed V0, V1, V2, and V3) (Wight, 2002). In order to validate the up-regulation of versican we designed isoform-specific primers to estimate the levels of induction of each splice form (Fig. 2A). For the remaining genes, one single set of primers was used after optimization of real-time PCR parameters. Independent real-time RT-PCR assays were performed in triplicate, and the means ± SEM of the relative expression levels are shown in Fig. 2. In all cases the up-regulation of the target genes is specific for SAOS-MAGP1B as indicated by the statistically significant (multiple-t test, $p<0.05$) differences between the average expression values in SAOS-MAGP1B cells relative to the SAOS-C line (Fig. 2). The expression values of the selected genes were in close agreement with the microarray values (Table 2), confirming the transcriptional profile obtained by the genechip analysis.

4. Discussion

The function of the intracellular MAGP1B splice variant is essentially unknown, besides the fact that its transient expression in rat lung fibroblasts induced changes in cell shape and reduced adhesion to the substrate (Segade et al., 2002). To gain insights into MAGP1B we

developed transfected cell lines derived form the human osteosarcoma cell line, SAOS-2. The choice of the host cell line was relatively straightforward based on i) absence of MAGP1 expression in native SAOS-2 cells; ii) since SAOS-2 cells deposit an extensive ECM (McQuillan et al., 1995) they must possess the molecular machinery for post-translational modification, secretion, and deposition of ECM proteins; and iii) some of the major components of the SAOS-2 ECM (e.g. decorin) (McQuillan et al., 1995) are relevant to MAGP1 biology (Trask et al., 2000).

Stress responses in cells that over-express exogenous gene products may confound the gene profiling analysis if they can not be separated from the genuine effect of MAGP1B. To minimize the problem we followed a three-pronged approach. First, all the RNA sources for gene profiling and validation were G418-selected transfected cells and no untransfected SAOS-2 cells were used. It is a reasonable assumption that any transfection-induced stress would be similar in the three derived lines. Second, a generalized stress response to over-expression of heterologous proteins is expected to be qualitatively similar in the three lines. This is due to the fact that all lines, including SAOS-C transfected with the empty vector, over-express at least the Neomycin Resistance (neo) gene product required for G418 selection. Third, gene changes that were quantitatively similar in both SAOS-MAGP1A and SAOS-MAGP1B were subtracted from the results in order to identify genes uniquely altered in the SAOS-MAGP1B line. In this manner we are confident that our results only show the real biological effects of MAGP1B.

The analysis of the genechip results showed that the gene with the highest fold increase is CSPG2, encoding the chondroitin sulfate proteoglycan, versican, a component of the ECM of soft tissues (Wight, 2002). The four versican splice forms (V0, V1, V2, and V3) differ in the number of glycosaminoglycan attachment sites that determine the functional specificities of the variants as much as their protein sequence (Wight, 2002). Thus, V1 promotes cell growth and inhibits the expression of the proapoptotic protein Bad, whereas the V2 form diminishes cell growth and is not antiapoptotic (Sheng et al., 2005). Versican V3 slows melanoma cell proliferation and augments cell adhesion and migration (Serra et al., 2005). Interestingly, versican is found associated to the microfibrils through its interaction with fibrillin-1 (Isogai et al., 2002). Versican is not simply a structural component of the elastic fibers. In smooth muscle cells, over-expression of versican V3 enhances cell adhesion, decreases cell proliferation, and up-regulates tropoelastin expression both at the mRNA level and as deposited elastin (Merrilees et al., 2002). In fibroblasts that are genetically deficient in the formation of elastic fibers, overexpression of versican V3 reverses the impairment in elastogenesis and restores the formation of normal elastic laminae (Hinek et al., 2004).

CDC42 Effector Protein 3 (CDC42EP3, also known as CEP3 or Borg2) (Hirsch et al., 2001; Joberty et al., 1999) binds to the small GTPases CDC42 and TC10 that regulate cytoskeleton activity, cell adhesion and migration. The CDC42EP proteins may act downstream of CDC42/TC10 to induce actin filament assembly that leads to cell shape changes (Hirsch et al., 2001), through their interaction with the septin GTPases (Joberty et al., 2001). The closely related CDC42EP5 (Borg3) causes a delay in cell spreading (Joberty et al., 1999).

The product of the ITGA4 gene, Integrin α4, is mainly involved in cell adhesion. Thus, α4β1 integrin and its ligand VCAM1 mediate a critical cell adhesion event for the survival of endothelial cells (Garmy-Susini et al., 2005). But α4β1 also promotes lamellipodia protrusion (Pinco et al., 2002) and is essential for the migration of progenitor cells to form the heart epicardium (Sengbusch et al., 2002). Cells expressing Integrin α4, also known as VLA4, are resistant to apoptosis from loss of anchorage mediated by the PI3K/Akt/Bcl2 pathway (Matsunaga et al., 2003). Interestingly, AKT1 is up-regulated by MAGP1B in our microarray data (Table 2).

The biology of MAGP1, with its extra- and intracellular facets, is reminiscent of the extracellular components known as matricellular proteins. These are proteins that interact with cell-surface receptors, ECM, growth factors, and/or proteases, but do not themselves serve strictly or exclusively structural roles (Bornstein and Sage, 2002). Among the better known matricellular proteins are SPARC, thrombospondin, tenascin C, tenascin X, syndecans, and osteopontin (Bornstein and Sage, 2002). Like SPARC, MAGP1, through its secreted MAGP1A variant, interacts with a number of ECM components (e.g., fibrillin, elastin, collagen IV, and decorin) but it is not itself a structural element of the microfibril. On the other hand, MAGP1 shows important differences with the matricellular proteins. Matricellular proteins act extracellularly to modulate cell-cell and cell-matrix interactions. However, MAGP1 expresses a *strictly intracellular* form, MAGP1B. This suggests instead that MAGP1 is functionally closer to a heterogeneous collection of molecules known as intracrine mediators that function inside the cell after internalization or through retention in their cells of synthesis (Re and Cook, 2006). Intracrins are structurally heterogeneous, mainly growth regulatory, related to angiogenesis, sometimes located to the nucleus, and synthesized as multiple isoforms (Re and Cook, 2006). A recent review on intracrins (Re and Cook, 2006) does not include extracellular matrix components, but while an intracellular role by a microfibril-associated protein is unusual, there are interesting and important precedents for matrix proteins that also function inside the cell. Lysyl oxidase is a secreted, extracellular protein that catalyzes the formation of covalent crosslinks in collagen and elastin. An enzymatically active form has been detected in the nucleus of rat vascular smooth muscle cells, where it acts as a suppressor of transformation by the Ras gene product (Kenyon et al., 1991; Nellaiappan et al., 2000).

Since the number of genes in the genome is limited, alternative splicing provides a mechanism to increase the diversity of the proteome together with a more flexible and complex regulation of cell processes. Alternatively spliced transcripts are prevalent among genes that code for extracellular matrix proteins, since many of the large structural proteins are formed by combinations of discrete structural domains present in a variable number of copies (Boyd et al., 1993). The multiple splice forms of fibronectin (Schwarzbauer, 1991), latent TGFβ-binding proteins (Oklu and Hesketh, 2000), and laminins (Tunggal et al., 2000) are well-characterized examples of how isoforms differ in their functions. Moreover, alternative splicing is an efficient process to generate dual-role proteins through the inclusion or exclusion of exon modules that results in changes in localization or function (Stamm et al., 2005). We envision a regulatory mechanism which, by controlling the ratio of splicing between MAGP1A and MAGP1B, links ECM deposition, in which extracellular MAGP1A participates, with cellular processes that prime the cell for ECM assembly through the MAGP1B-responsive genes.

In this view, MAGP1B represents a unique form of matricellular protein, one whose function is entirely carried out within the cell, although “derived” from an ECM protein. Taken together, our data uncovered a critical role of MAGP1B that should contribute towards the elucidation of the regulation of ECM assembly.

Acknowledgements

This work was supported by NIH Grant HL071960 (R.P.M.) and by the WFUSM Center for Human Genomics (F.S.). We are grateful to Dax Allred (WFUSM) for his technical support and to Dr. Elisabeth Burton (Penn SDM) for her assistance with microscopy.

References

Bornstein P, Sage EH. Matricellular proteins: extracellular modulators of cell function. Curr Opin Cell Biol 2002;14:608–16. [PubMed: 12231357]

Boyd CD, Pierce RA, Schwarzbauer JE, Doege K, Sandell LJ. Alternate exon usage is a commonly used mechanism for increasing coding diversity within genes coding for extracellular matrix proteins. Matrix 1993;13:457–69. [PubMed: 8309425]

Brown-Augsburger P, Broekelmann T, Mecham L, Mercer R, Gibson MA, Cleary EG, Abrams WR, Rosenbloom J, Mecham RP. Microfibril-associated glycoprotein binds to the carboxyl-terminal domain of tropoelastin and is a substrate for transglutaminase. J Biol Chem 1994;269:28443–9. [PubMed: 7961786]

Charbonneau NL, Ono RN, Corson GM, Keene DR, Sakai LY. Fine tuning of growth factor signals depends on fibrillin microfibril networks. Birth Defects Res C Embryo Today 2004;72:37–50. [PubMed: 15054903]

Chen Y, Faraco J, Yin W, Germiller J, Francke U, Bonadio J. Structure, chromosomal localization, and expression pattern of the murine Magp gene. J Biol Chem 1993;268:27381–9. [PubMed: 8262979]

Chomczynski P, Sacchi N. Single-step method of RNA isolation by acid guanidinium thiocyanate-phenol-chloroform extraction. Anal Biochem 1987;162:156–9. [PubMed: 2440339]

Cobb LM, Mychaleckyj JC, Wozniak DJ, Lopez-Boado YS. Pseudomonas aeruginosa flagellin and alginate elicit very distinct gene expression patterns in airway epithelial cells: implications for cystic fibrosis disease. J Immunol 2004;173:5659–70. [PubMed: 15494517]

Faraco J, Bashir M, Rosenbloom J, Francke U. Characterization of the human gene for microfibril-associated glycoprotein (MFAP2), assignment to chromosome 1p36.1–p35, and linkage to D1S170. Genomics 1995;25:630–7. [PubMed: 7759096]

Finnis ML, Gibson MA. Microfibril-associated glycoprotein-1 (MAGP-1) binds to the pepsin-resistant domain of the α3(VI) chain of type VI collagen. J Biol Chem 1997;272:22817–23. [PubMed: 9278443]

Fogh J, Fogh JM, Orfeo T. One hundred and twenty-seven cultured human tumor cell lines producing tumors in nude mice. J Natl Cancer Inst 1977;59:221–6. [PubMed: 327080]

Garmy-Susini B, Jin H, Zhu Y, Sung RJ, Hwang R, Varner J. Integrin α4β1-VCAM-1-mediated adhesion between endothelial and mural cells is required for blood vessel maturation. J Clin Invest 2005;115:1542–51. [PubMed: 15902308]

Gibson MA, Sandberg LB, Grosso LE, Cleary EG. Complementary DNA cloning establishes microfibril-associated glycoprotein (MAGP) to be a discrete component of the elastin-associated microfibrils. J Biol Chem 1991;266:7596–601. [PubMed: 2019589]

Harris MA, Clark J, Ireland A, Lomax J, Ashburner M, Foulger R, et al. The Gene Ontology (GO) database and informatics resource. Nucleic Acids Res 2004;32:D258–61. [PubMed: 14681407]

Hinek A, Braun KR, Liu K, Wang Y, Wight TN. Retrovirally mediated overexpression of versican v3 reverses impaired elastogenesis and heightened proliferation exhibited by fibroblasts from Costello syndrome and Hurler disease patients. Am J Pathol 2004;164:119–31. [PubMed: 14695326]

Hirsch DS, Pirone DM, Burbelo PD. A new family of Cdc42 effector proteins, CEPs, function in fibroblast and epithelial cell shape changes. J Biol Chem 2001;276:875–83. [PubMed: 11035016]

Isogai Z, Aspberg A, Keene DR, Ono RN, Reinhardt DP, Sakai LY. Versican interacts with fibrillin-1 and links extracellular microfibrils to other connective tissue networks. J Biol Chem 2002;277:4565–72. [PubMed: 11726670]

Joberty G, Perlungher RR, Macara IG. The Borgs, a new family of Cdc42 and TC10 GTPase-interacting proteins. Mol Cell Biol 1999;19:6585–97. [PubMed: 10490598]

Joberty G, Perlungher RR, Sheffield PJ, Kinoshita M, Noda M, Haystead T, Macara IG. Borg proteins control septin organization and are negatively regulated by Cdc42. Nat Cell Biol 2001;3:861–6. [PubMed: 11584266]

Karolchik D, Baertsch R, Diekhans M, Furey TS, Hinrichs A, Lu YT, et al. The UCSC Genome Browser Database. Nucleic Acids Res 2003;31:51–4. [PubMed: 12519945]

Kenyon K, Contente S, Trackman PC, Tang J, Kagan HM, Friedman RM. Lysyl oxidase and rrg messenger RNA. Science 1991;253:802. [PubMed: 1678898]

Livak KJ, Schmittgen TD. Analysis of relative gene expression data using real–time quantitative PCR and the $2^{(-Ct)}$ Method. Methods 2001;25:402–8. [PubMed: 11846609]

Matsunaga T, Takemoto N, Sato T, Takimoto R, Tanaka I, Fujimi A, et al. Interaction between leukemic-cell VLA-4 and stromal fibronectin is a decisive factor for minimal residual disease of acute myelogenous leukemia. Nat Med 2003;9:1158–65. [PubMed: 12897778]

McQuillan DJ, Richardson MD, Bateman JF. Matrix deposition by a calcifying human osteogenic sarcoma cell line (SAOS-2). Bone 1995;16:415–26. [PubMed: 7605701]

Mecham, RP.; Davis, EC. Extracellular Matrix assembly and structure. Yurchenko, PD.; Mecham, RP., editors. Academic Press; San Diego: 1994.

Merrilees MJ, Lemire JM, Fischer JW, Kinsella MG, Braun KR, Clowes AW, Wight TN. Retrovirally mediated overexpression of versican v3 by arterial smooth muscle cells induces tropoelastin synthesis and elastic fiber formation in vitro and in neointima after vascular injury. Circ Res 2002;90:481–7. [PubMed: 11884379]

Miyamoto A, Lau R, Hein PW, Shipley JM, Weinmaster G. Microfibrillar proteins MAGP-1 and MAGP-2 induce Notch1 extracellular domain dissociation and receptor activation. J Biol Chem 2006;281:10089–97. [PubMed: 16492672]

Nellaiappan K, Risitano A, Liu G, Nicklas G, Kagan HM. Fully processed lysyl oxidase catalyst translocates from the extracellular space into nuclei of aortic smooth-muscle cells. J Cell Biochem 2000;79:576–82. [PubMed: 10996848]

Oklu R, Hesketh R. The latent transforming growth factor beta binding protein (LTBP) family. Biochem J 2000;352(Pt 3):601–10. [PubMed: 11104663]

Pinco KA, He W, Yang JT. α4β1 integrin regulates lamellipodia protrusion via a focal complex/focal adhesion-independent mechanism. Mol Biol Cell 2002;13:3203–17. [PubMed: 12221126]

Re RN, Cook JL. The intracrine hypothesis: an update. Regul Pept 2006;133:1–9. [PubMed: 16226324]

Reinboth B, Hanssen E, Cleary EG, Gibson MA. Molecular interactions of biglycan and decorin with elastic fiber components: biglycan forms a ternary complex with tropoelastin and microfibril-associated glycoprotein 1. J Biol Chem 2002;277:3950–7. [PubMed: 11723132]

Robinson PN, Godfrey M. The molecular genetics of Marfan syndrome and related microfibrillopathies. J Med Genet 2000;37:9–25. [PubMed: 10633129]

Sakamoto H, Broekelmann T, Cheresh DA, Ramirez F, Rosenbloom J, Mecham RP. Cell-type specific recognition of RGD- and non-RGD-containing cell binding domains in fibrillin-1. J Biol Chem 1996;271:4916–22. [PubMed: 8617764]

Schwarzbauer JE. Alternative splicing of fibronectin: three variants, three functions. Bioessays 1991;13:527–33. [PubMed: 1755828]

Segade F, Broekelmann TJ, Pierce RA, Mecham RP. Revised genomic structure of the human MAGP1 gene and identification of alternate transcripts in human and mouse tissues. Matrix Biol 2000;19:671–82. [PubMed: 11102756]

Segade F, Trask BC, Broekelmann TJ, Pierce RA, Mecham RP. Identification of a matrix-binding domain in MAGP1 and MAGP2 and intracellular localization of alternative splice forms. J Biol Chem 2002;277:11050–7. [PubMed: 11796718]

Sengbusch JK, He W, Pinco KA, Yang JT. Dual functions of [alpha]4[beta]1 integrin in epicardial development: initial migration and long-term attachment. J Cell Biol 2002;157:873–82. [PubMed: 12021259]

Serra M, Miquel L, Domenzain C, Docampo MJ, Fabra A, Wight TN, Bassols A. V3 versican isoform expression alters the phenotype of melanoma cells and their tumorigenic potential. Int J Cancer 2005;114:879–86. [PubMed: 15645431]

Sheng W, Wang G, Wang Y, Liang J, Wen J, Zheng PS, Wu Y, Lee V, Slingerland J, Dumont D, Yang BB. The roles of versican V1 and V2 isoforms in cell proliferation and apoptosis. Mol Biol Cell 2005;16:1330–40. [PubMed: 15635104]

Stamm S, Ben-Ari S, Rafalska I, Tang Y, Zhang Z, Toiber D, Thanaraj TA, Soreq H. Function of alternative splicing. Gene 2005;344:1–20. [PubMed: 15656968]

Takagaki Y, MacDonald CC, Shenk T, Manley JL. The human 64-KDa polyadenylylation factor contains a ribonucleoprotein-type RNA binding domain and unusual auxiliary motifs. Proc Natl Acad Sci USA 1992;89:1403–1407. [PubMed: 1741396]

Trask BC, Trask TM, Broekelmann T, Mecham RP. The microfibrillar proteins MAGP-1 and fibrillin-1 form a ternary complex with the chondroitin sulfate proteoglycan decorin. Mol Biol Cell 2000;11:1499–507. [PubMed: 10793130]

Tunggal P, Smyth N, Paulsson M, Ott MC. Laminins: structure and genetic regulation. Microsc Res Tech 2000;51:214–27. [PubMed: 11054872]

Wang X, Seed B. A PCR primer bank for quantitative gene expression analysis. Nucleic Acids Res 2003;31:e154. [PubMed: 14654707]

Werneck CC, Trask BC, Broekelmann TJ, Trask TM, Ritty TM, Segade F, Mecham RP. Identification of a major microfibril-associated glycoprotein-1-binding domain in fibrillin-2. J Biol Chem 2004;279:23045–51. [PubMed: 15044481]

Wight TN. Versican: a versatile extracellular matrix proteoglycan in cell biology. Curr Opin Cell Biol 2002;14:617–23. [PubMed: 12231358]

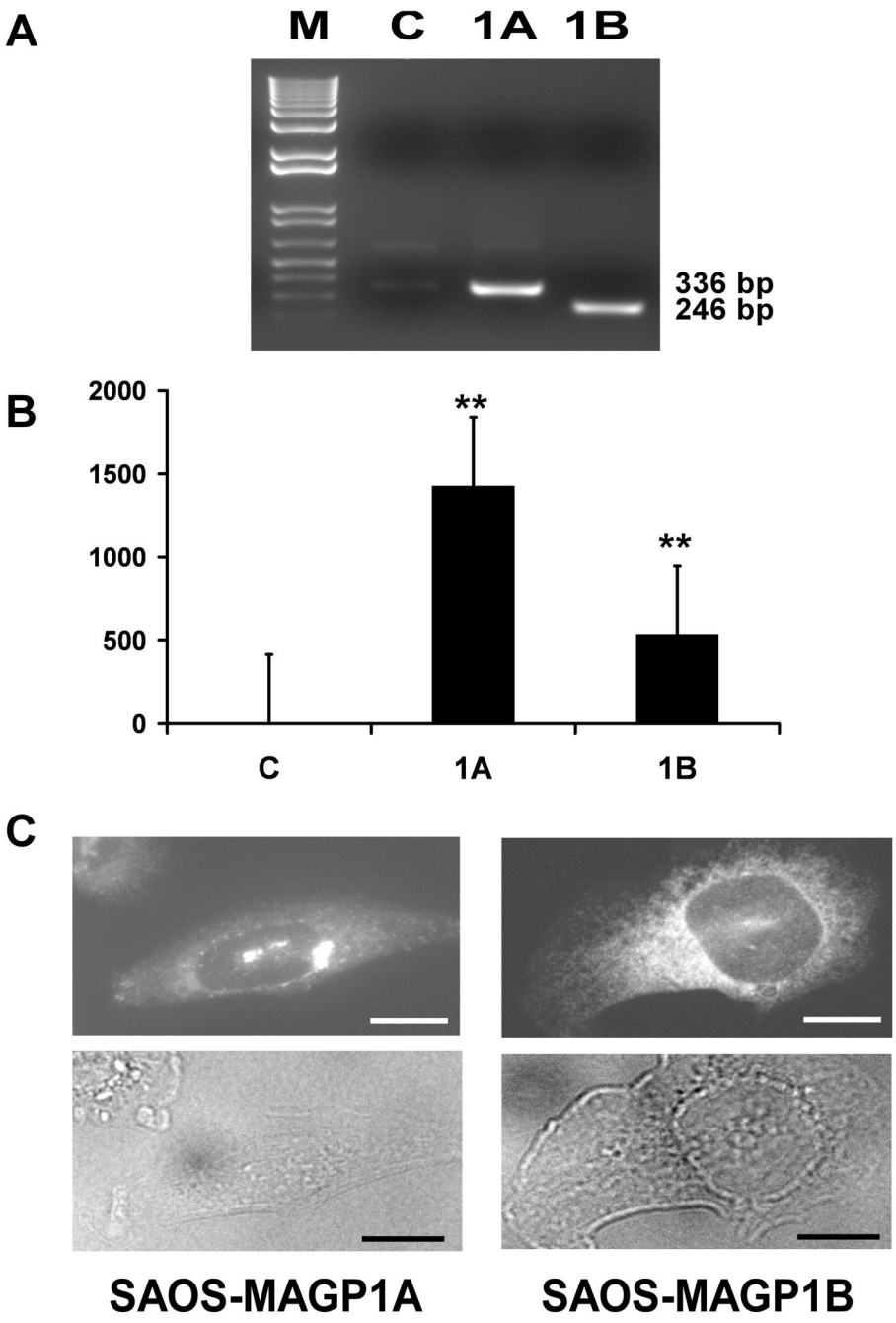

Fig. 1.

A. Expression of human MAGP1A and MAGP1B transcripts in transfected SAOS cell lines by conventional RT-PCR. PCR was performed with oligonucleotides located in exons 2 (HM5) and 6 (HM3) using template cDNA from SAOS-C (lane C), SAOS-MAGP1A (lane 1A), or SAOS-MAGP1B (lane 1B). The sizes of the indicated bands are 336 bp for MAGP1A and 246 bp for MAGP1B. M, 100-bp DNA ladder standard. B. Quantitation of the expression levels of isoform mRNAs by real-time RT-PCR with SYBR Green detection chemistry. Relative levels of transcripts are normalized to the level in SAOS-C. **, p-value <0.01 for pairwise comparison to SAOS-C by t-test analysis. C. Distribution patterns of the MAGP1 splice variants in stably-transfected SAOS cell lines. Cells were fixed, and subjected to indirect immunofluorescence

detection of human MAGP1A-V5 (left panel, upper image) or MAGP1B-V5 (right panel, upper image) with monoclonal anti-V5 antibodies. Secondary antibodies were Alexa 488-conjugated goat anti-mouse. Phase contrast micrographs showing the morphology of the immunostained cells (lower images). Images were acquired with a ×40 objective at a final optical magnification of ×400. Horizontal bars, 10 μm.

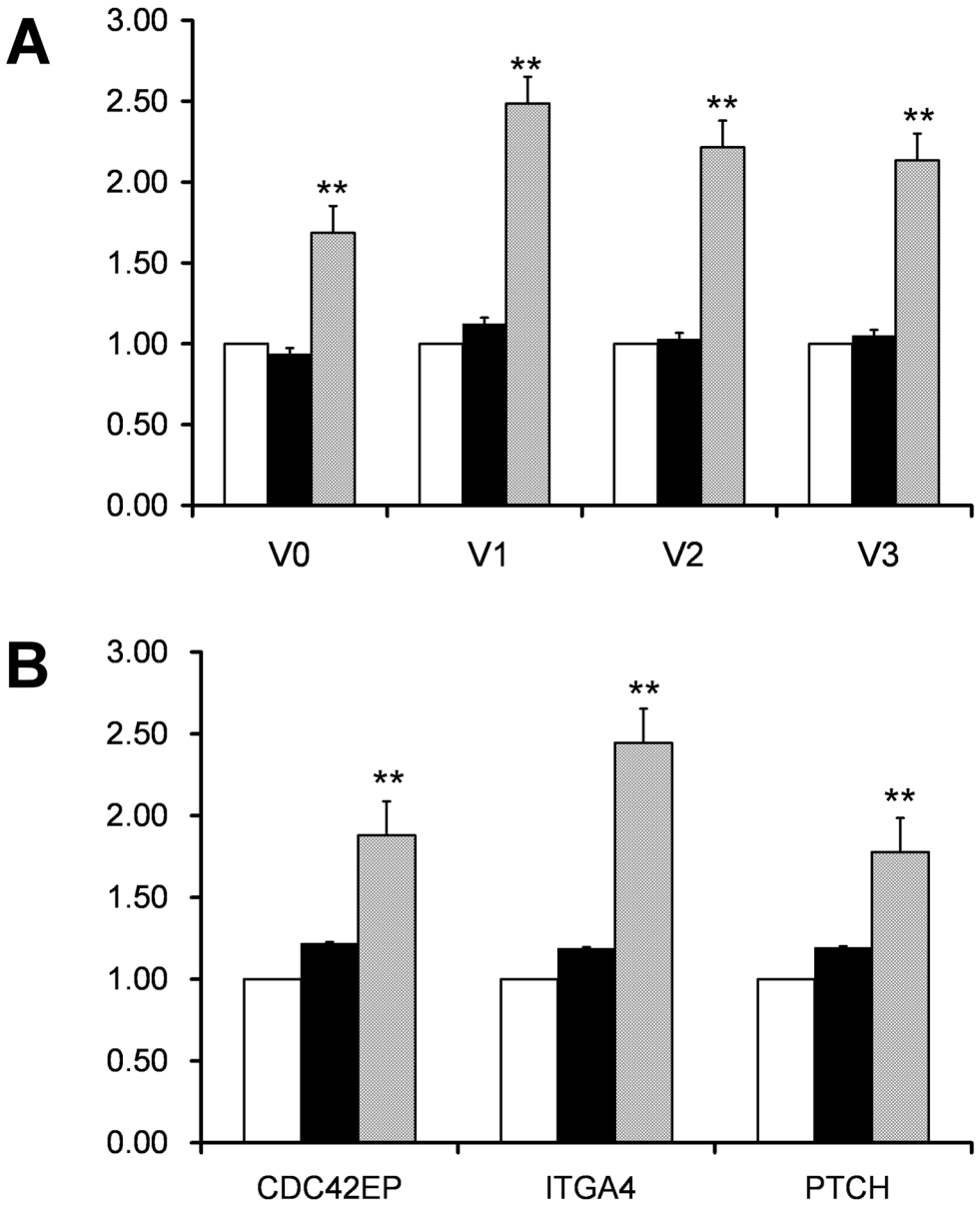

Fig. 2.

Validation of selected gene mRNA levels in SAOS-2 MAGP1-transfected cells by real-time RT-PCR. PCR was performed with oligonucleotide primer pairs described in Table 1 using template cDNA from SAOS-C (empty box), SAOS-MAGP1A (black box), or SAOS-MAGP1B (stippled box) with SYBR Green detection chemistry. A, Relative levels of alternate splice forms of versican. B, Relative levels of CDC42EP3, ITGA4, and PTCH. **, p-value <0.01 for pairwise comparison to SAOS-C by t-test analysis.

Table 1

Primers used for real-time PCR validation of selected genes

Gene	Sense	Antisense	Target size (bp)
MFAP2	ACCTCTTCCTGCTATTCCTGCCTG	CACTGTTTGCAAGGCCTGTGTATG	336/246[a]
CSPG2 V0	GCACAAAATTTCACCCTGACAT	CTGAATCTATTGGATGACCAATTACAC	105
CSPG2 V1	CCCAGTGTGGAGGTGGTCTACT	CACTCAAATCACTCATTCGACGTT	122
CSPG2 V2	GCACAAAATTTCACCCTGACATT	TGCATACGTAGGAAGTTTCAGTAG	133
CSPG2 V3	CCCTCCCCCTGATAGCAGAT	GGCACGGGTTCATTTTGC	69
CDC42EP3	AAGACCCCAATTTACCTGAAAGC	TGGCGAAAGTCTCCAAGCG	110
ITGA4	ATTTTCGGAGCCAGCATACTAC	AGAAGCCATCTGCATTGAGGT	150
PTCH	AGTTCACCGTTCACGTTGCTTTGG	CGCCAGCACAGCAAAGAAATACCT	188
CAV2	ATGAAGCTCATATCCTTTTGAAGGT	ATGAATTCCGAGAAGTCTGCTCAT	550

[a] Amplicon sizes derived from MAGP1A or MAGP1B, respectively.

Table 2

Genes exclusively regulated by MAGP1B

Gene name	Gene Symbol	GenBank accession	Peak ratio
Upregulated (67 genes)			
Development			
Versican	CSPG2	NM_004385	2.76
Patched	PTCH	NM_000264	2.00
Short stature homeobox 2	SHOX2	NM_006884	1.60
Notch homolog 2	NOTCH2	NM_018067	1.57
Reticulon 3	RTN3	NM_201430	1.53
Dickkopf homolog 1	DKK1	NM_012242	1.53
Prominin 1	PROM1	NM_006017	1.53
Signal transduction			
CDC42 effector protein 3	CDC42EP	NM_006449	2.43
Development and differentiation enhancing factor 1	DDEF1	NM_018482	1.83
Prune homolog	PRUNE	NM_021222	1.64
TRAF family member-associated NF-κB activator	TANK	NM_133484	1.62
Putative NF-κB activating protein 373	FLJ23091	NM_024911	1.58
Neurofibromin 1	NF1	NM_000267	1.54
Akt-1	AKT1	NM_014573	1.52
Phospholipase C, γ1	PLCG1	NM_182811	1.52
Cell adhesion			
Integrin α4	ITGA4	NM_000885	2.15
Structural			
Kinesin 1B	KIF1B	NM_183416	2.00
Myosin X	MYO10	NM_012334	2.00
Echinoderm microtubule associated protein-like 1	EML4	NM_019063	1.90
Spectrin β, non-erythrocytic 1	SPTBN1	NM_178313	1.88
Dynactin 1	DCTN1	NM_023019	1.83
Plastin 3, T isoform	PLS3	NM_005032	1.58
Dynein, cytoplasmic, heavy polypeptide 1	DNCH1	NM_001376	1.54
Gene expression			
Special AT-rich sequence-binding protein 2	SATB2	NM_015265	1.94
C-terminal binding protein 1	CTBP1	NM_001328	1.89
SREBP cleavage-activating protein	SCAP	NM_183063	1.69
MYST histone acetyltransferase 2	MYST2	NM_007067	1.60
Protein phosphatase 1 regulatory inhibitor	PPP1R8	NM_138558	1.57
Distal-less homeo box 2	DLX2	NM_004405	1.57
Transcription factor 7	TCF7	NM_201634	1.56
Calreticulin	CALR	NM_004343	1.52
Translation initiation factor 4γ, 1	EIF4G1	NM_198242	1.52
Tumor-related			
Sarcoma antigen NY-SAR-91	FLJ11730	NM_022756	1.94
Glycoprotein (transmembrane) nmb	GPNMB	NM_002510	1.88
Papillary renal carcinoma translocation-associated	PRCC	NM_199416	1.77
Serologically defined colon cancer antigen 3	SDCCAG3	NM_006643	1.60
Metabolism			
Cytochrome c oxidase subunit VIIc	COX7C	NM_001867	1.90
Acyl-CoA synthetase long-chain family member 1	ACSL1	NM_001995	1.84
Phosphoserine phosphatase	PSPH	NM_004577	1.83
Aldehyde dehydrogenase 1 family, member 3	ALDH1A3	NM_018446	1.76
Glyosyltransferase 8 domain containing 1	GLT8D1	NM_152932	1.75
Nicotinamide nucleotide transhydrogenase	NNT	NM_182977	1.70
Thioesterase superfamily member 2	THEM2	NM_018473	1.60
Pyruvate dehydrogenase β	PDHB	NM_000925	1.55
Phosphoribosylformylglycininamide synthase	PFAS	NM_012393	1.54
GlcNAc-1-P-transferase	DPAGT1	NM_203316	1.51

Gene name	Gene Symbol	GenBank accession	Peak ratio
Hormone response			
Growth hormone receptor	GHR	NM_000163	1.88
Protein metabolism			
Carboxypeptidase E	CPE	NM_001873	1.74
Ring finger protein 7	RNF7	NM_183237	1.67
Down syndrome critical region gene 5	DSCR5	NM_153682	1.57
Ubiquitin-conjugating enzyme E2L member 3	UBE2L3	NM_198157	1.54
Transport			
SEC31-like 1	SEC31L1	NM_016211	1.71
Adaptin ear-binding coat-associated protein 1	NECAP1	NM_015509	1.62
Uncharacterized gene product			
Chromosome 11 open reading frame 8	C11orf8	NM_001584	2.31
Hypothetical protein HSPC132	HSPC132	NM_016399	2.01
KIAA0367	KIAA0367	XM_041018	1.93
KIAA0657	KIAA0657	XM_051017	1.93
Differential display and activated by p53	DDA3	NM_032636	1.70
YLP motif containing 1	YLPM1	XM_085151	1.67
Hypothetical protein MGC3032	MGC3032	N/A	1.64
Hypothetical protein FLJ10350	FLJ10350	NM_018067	1.58
Chromosome 22 open reading frame 9	C22orf9	NM_015264	1.55
La-related protein	LARP	NM_015315	1.53
Zinc finger, CW type, coiled coil domain 1	ZCWCC1	NM_014941	1.53
KIAA0251 protein	KIAA0251	NM_015027	1.53
Hypothetical protein MAC30	MAC30	NM_014573	1.52
Family with sequence similarity 46, member A	FAM46A	NM_017633	1.51
Downregulated (8 genes)			
Gene expression			
Cleavage stimulation factor, 3′ pre-RNA, subunit 2	CSTF2	NM_001325	0.55
Retinoic acid receptor responder 3	RARRES3	NM_004585	0.65
Protein modification			
Ubquitin specific protease 5 (isopeptidase T)	USP5	NM_003481	0.60
Cell adhesion			
Integrin-binding sialoprotein	IBSP	NM_004967	0.63
Signal transduction			
CAP, adenylate cyclase-associated protein 1	CAP1	NM_006367	0.64
Transport			
Adaptor-related protein complex 1, σ 1 subunit	AP1S1	NM_057089	0.67
Uncharacterized gene product			
Breast carcinoma amplified sequence 3	BCAS3	NM_017679	0.53
DKFZP547E1010 protein	N/A	NM_015607	0.64

Genes with differentially changed expression in SAOS-MAGP1B cells when compared with SAOS-MAGP1A and SAOS-C cells sorted into the Upregulated or down-regulated categories. In the table, gene ontology category, gene name, gene symbol (or gene ID), the accession number and peak ratio are provided. Genes with a ≥1.5-fold change were considered as differentially regulated using human U133A oligonucleotide arrays.